

Measurement of time-dependent CP asymmetry in $B^0 \rightarrow K_S^0 \pi^0 \gamma$ decays

B. Aubert,¹ M. Bona,¹ Y. Karyotakis,¹ J. P. Lees,¹ V. Poireau,¹ E. Prencipe,¹ X. Prudent,¹ V. Tisserand,¹ J. Garra Tico,² E. Grauges,² L. Lopez,^{3a,3b} A. Palano,^{3a,3b} M. Pappagallo,^{3a,3b} G. Eigen,⁴ B. Stugu,⁴ L. Sun,⁴ G. S. Abrams,⁵ M. Battaglia,⁵ D. N. Brown,⁵ R. N. Cahn,⁵ R. G. Jacobsen,⁵ L. T. Kerth,⁵ Yu. G. Kolomensky,⁵ G. Lynch,⁵ I. L. Osipenkov,⁵ M. T. Ronan,^{5,*} K. Tackmann,⁵ T. Tanabe,⁵ C. M. Hawkes,⁶ N. Soni,⁶ A. T. Watson,⁶ H. Koch,⁷ T. Schroeder,⁷ D. Walker,⁸ D. J. Asgeirsson,⁹ B. G. Fulsom,⁹ C. Hearty,⁹ T. S. Mattison,⁹ J. A. McKenna,⁹ M. Barrett,¹⁰ A. Khan,¹⁰ V. E. Blinov,¹¹ A. D. Bukin,¹¹ A. R. Buzykaev,¹¹ V. P. Druzhinin,¹¹ V. B. Golubev,¹¹ A. P. Onuchin,¹¹ S. I. Serednyakov,¹¹ Yu. I. Skovpen,¹¹ E. P. Solodov,¹¹ K. Yu. Todyshev,¹¹ M. Bondioli,¹² S. Curry,¹² I. Eschrich,¹² D. Kirkby,¹² A. J. Lankford,¹² P. Lund,¹² M. Mandelkern,¹² E. C. Martin,¹² D. P. Stoker,¹² S. Abachi,¹³ C. Buchanan,¹³ J. W. Gary,¹⁴ F. Liu,¹⁴ O. Long,¹⁴ B. C. Shen,^{14,*} G. M. Vitug,¹⁴ Z. Yasin,¹⁴ L. Zhang,¹⁴ V. Sharma,¹⁵ C. Campagnari,¹⁶ T. M. Hong,¹⁶ D. Kovalskyi,¹⁶ M. A. Mazur,¹⁶ J. D. Richman,¹⁶ T. W. Beck,¹⁷ A. M. Eisner,¹⁷ C. J. Flacco,¹⁷ C. A. Heusch,¹⁷ J. Kroseberg,¹⁷ W. S. Lockman,¹⁷ T. Schalk,¹⁷ B. A. Schumm,¹⁷ A. Seiden,¹⁷ L. Wang,¹⁷ M. G. Wilson,¹⁷ L. O. Winstrom,¹⁷ C. H. Cheng,¹⁸ D. A. Doll,¹⁸ B. Echenard,¹⁸ F. Fang,¹⁸ D. G. Hitlin,¹⁸ I. Narsky,¹⁸ T. Piatenko,¹⁸ F. C. Porter,¹⁸ R. Andreassen,¹⁹ G. Mancinelli,¹⁹ B. T. Meadows,¹⁹ K. Mishra,¹⁹ M. D. Sokoloff,¹⁹ P. C. Bloom,²⁰ W. T. Ford,²⁰ A. Gaz,²⁰ J. F. Hirschauer,²⁰ M. Nagel,²⁰ U. Nauenberg,²⁰ J. G. Smith,²⁰ K. A. Ulmer,²⁰ S. R. Wagner,²⁰ R. Ayad,^{21,+} A. Soffer,^{21,‡} W. H. Toki,²¹ R. J. Wilson,²¹ D. D. Altenburg,²² E. Feltresi,²² A. Hauke,²² H. Jasper,²² M. Karbach,²² J. Merkel,²² A. Petzold,²² B. Spaan,²² K. Wacker,²² M. J. Kobel,²³ W. F. Mader,²³ R. Nogowski,²³ K. R. Schubert,²³ R. Schwierz,²³ J. E. Sundermann,²³ A. Volk,²³ D. Bernard,²⁴ G. R. Bonneaud,²⁴ E. Latour,²⁴ Ch. Thiebaux,²⁴ M. Verderi,²⁴ P. J. Clark,²⁵ W. Gradl,²⁵ S. Playfer,²⁵ J. E. Watson,²⁵ M. Andreotti,^{26a,26b} D. Bettoni,^{26a} C. Bozzi,^{26a} R. Calabrese,^{26a,26b} A. Cecchi,^{26a,26b} G. Cibinetto,^{26a,26b} P. Franchini,^{26a,26b} E. Luppi,^{26a,26b} M. Negrini,^{26a,26b} A. Petrella,^{26a,26b} L. Piemontese,^{26a} V. Santoro,^{26a,26b} R. Baldini-Ferroli,²⁷ A. Calcaterra,²⁷ R. de Sangro,²⁷ G. Finocchiaro,²⁷ S. Pacetti,²⁷ P. Patteri,²⁷ I. M. Peruzzi,^{27,§} M. Piccolo,²⁷ M. Rama,²⁷ A. Zallo,²⁷ A. Buzzo,^{28a} R. Contri,^{28a,28b} M. Lo Vetere,^{28a,28b} M. M. Macri,^{28a} M. R. Monge,^{28a,28b} S. Passaggio,^{28a} C. Patrignani,^{28a,28b} E. Robutti,^{28a} A. Santroni,^{28a,28b} S. Tosi,^{28a,28b} K. S. Chaisanguanthum,²⁹ M. Morii,²⁹ J. Marks,³⁰ S. Schenk,³⁰ U. Uwer,³⁰ V. Klose,³¹ H. M. Lacker,³¹ D. J. Bard,³² P. D. Dauncey,³² J. A. Nash,³² W. Panduro Vazquez,³² M. Tibbetts,³² P. K. Behera,³³ X. Chai,³³ M. J. Charles,³³ U. Mallik,³³ J. Cochran,³⁴ H. B. Crawley,³⁴ L. Dong,³⁴ W. T. Meyer,³⁴ S. Prell,³⁴ E. I. Rosenberg,³⁴ A. E. Rubin,³⁴ Y. Y. Gao,³⁵ A. V. Gritsan,³⁵ Z. J. Guo,³⁵ C. K. Lae,³⁵ A. G. Denig,³⁶ M. Fritsch,³⁶ G. Schott,³⁶ N. Arnaud,³⁷ J. Béquilleux,³⁷ A. D'Orazio,³⁷ M. Davier,³⁷ J. Firmino da Costa,³⁷ G. Grosdidier,³⁷ A. Höcker,³⁷ V. Lepeltier,³⁷ F. Le Diberder,³⁷ A. M. Lutz,³⁷ S. Pruvot,³⁷ P. Roudeau,³⁷ M. H. Schune,³⁷ J. Serrano,³⁷ V. Sordini,^{37,||} A. Stocchi,³⁷ G. Wormser,³⁷ D. J. Lange,³⁸ D. M. Wright,³⁸ I. Bingham,³⁹ J. P. Burke,³⁹ C. A. Chavez,³⁹ J. R. Fry,³⁹ E. Gabathuler,³⁹ R. Gamet,³⁹ D. E. Hutchcroft,³⁹ D. J. Payne,³⁹ C. Touramanis,³⁹ A. J. Bevan,⁴⁰ C. K. Clarke,⁴⁰ K. A. George,⁴⁰ F. Di Lodovico,⁴⁰ R. Sacco,⁴⁰ M. Sigamani,⁴⁰ G. Cowan,⁴¹ H. U. Flaecher,⁴¹ D. A. Hopkins,⁴¹ S. Paramesvaran,⁴¹ F. Salvatore,⁴¹ A. C. Wren,⁴¹ D. N. Brown,⁴² C. L. Davis,⁴² K. E. Alwyn,⁴³ D. Bailey,⁴³ R. J. Barlow,⁴³ Y. M. Chia,⁴³ C. L. Edgar,⁴³ G. Jackson,⁴³ G. D. Lafferty,⁴³ T. J. West,⁴³ J. I. Yi,⁴³ J. Anderson,⁴⁴ C. Chen,⁴⁴ A. Jawahery,⁴⁴ D. A. Roberts,⁴⁴ G. Simi,⁴⁴ J. M. Tuggle,⁴⁴ C. Dallapiccola,⁴⁵ X. Li,⁴⁵ E. Salvati,⁴⁵ S. Saremi,⁴⁵ R. Cowan,⁴⁶ D. Dujmic,⁴⁶ P. H. Fisher,⁴⁶ K. Koeneke,⁴⁶ G. Sciolla,⁴⁶ M. Spitznagel,⁴⁶ F. Taylor,⁴⁶ R. K. Yamamoto,⁴⁶ M. Zhao,⁴⁶ P. M. Patel,⁴⁷ S. H. Robertson,⁴⁷ A. Lazzaro,^{48a,48b} V. Lombardo,^{48a} F. Palombo,^{48a,48b} J. M. Bauer,⁴⁹ L. Cremaldi,⁴⁹ V. Eschenburg,⁴⁹ R. Godang,^{49,¶} R. Kroeger,⁴⁹ D. A. Sanders,⁴⁹ D. J. Summers,⁴⁹ H. W. Zhao,⁴⁹ M. Simard,⁵⁰ P. Taras,⁵⁰ F. B. Viaud,⁵⁰ H. Nicholson,⁵¹ G. De Nardo,^{52a,52b} L. Lista,^{52a} D. Monorchio,^{52a,52b} G. Onorato,^{52a,52b} C. Sciacca,^{52a,52b} G. Raven,⁵³ H. L. Snoek,⁵³ C. P. Jessop,⁵⁴ K. J. Knoepfel,⁵⁴ J. M. LoSecco,⁵⁴ W. F. Wang,⁵⁴ G. Benelli,⁵⁵ L. A. Corwin,⁵⁵ K. Honscheid,⁵⁵ H. Kagan,⁵⁵ R. Kass,⁵⁵ J. P. Morris,⁵⁵ A. M. Rahimi,⁵⁵ J. J. Regensburger,⁵⁵ S. J. Sekula,⁵⁵ Q. K. Wong,⁵⁵ N. L. Blount,⁵⁶ J. Brau,⁵⁶ R. Frey,⁵⁶ O. Igonkina,⁵⁶ J. A. Kolb,⁵⁶ M. Lu,⁵⁶ R. Rahmat,⁵⁶ N. B. Sinev,⁵⁶ D. Strom,⁵⁶ J. Strube,⁵⁶ E. Torrence,⁵⁶ G. Castelli,^{57a,57b} N. Gagliardi,^{57a,57b} M. Margoni,^{57a,57b} M. Morandin,^{57a} M. Posocco,^{57a} M. Rotondo,^{57a} F. Simonetto,^{57a,57b} R. Stroili,^{57a,57b} C. Voci,^{57a,57b} P. del Amo Sanchez,⁵⁸ E. Ben-Haim,⁵⁸ H. Briand,⁵⁸ G. Calderini,⁵⁸ J. Chauveau,⁵⁸ P. David,⁵⁸ L. Del Buono,⁵⁸ O. Hamon,⁵⁸ Ph. Leruste,⁵⁸ J. Ocariz,⁵⁸ A. Perez,⁵⁸ J. Prendki,⁵⁸ S. Sitt,⁵⁸ L. Gladney,⁵⁹ M. Biasini,^{60a,60b} R. Covarelli,^{60a,60b} E. Manoni,^{60a,60b} C. Angelini,^{61a,61b} G. Batignani,^{61a,61b} S. Bettarini,^{61a,61b} M. Carpinelli,^{61a,61b,**} A. Cervelli,^{61a,61b} F. Forti,^{61a,61b} M. A. Giorgi,^{61a,61b} A. Lusiani,^{61a,61c} G. Marchiori,^{61a,61b} M. Morganti,^{61a,61b} N. Neri,^{61a,61b} E. Paoloni,^{61a,61b} G. Rizzo,^{61a,61b} J. J. Walsh,^{61a} D. Lopes Pegna,⁶² C. Lu,⁶² J. Olsen,⁶² A. J. S. Smith,⁶² A. V. Telnov,⁶² F. Anulli,^{63a} E. Baracchini,^{63a,63b} G. Cavoto,^{63a} D. del Re,^{63a,63b} E. Di Marco,^{63a,63b} R. Faccini,^{63a,63b} F. Ferrarotto,^{63a} F. Ferroni,^{63a,63b} M. Gaspero,^{63a,63b} P. D. Jackson,^{63a} L. Li Gioi,^{63a}

M. A. Mazzone,^{63a} S. Morganti,^{63a} G. Piredda,^{63a} F. Polci,^{63a,63b} F. Renga,^{63a,63b} C. Voena,^{63a} M. Ebert,⁶⁴ T. Hartmann,⁶⁴ H. Schröder,⁶⁴ R. Waldi,⁶⁴ T. Adye,⁶⁵ B. Franek,⁶⁵ E. O. Olaiya,⁶⁵ F. F. Wilson,⁶⁵ S. Emery,⁶⁶ M. Escalier,⁶⁶ L. Esteve,⁶⁶ S. F. Ganzhur,⁶⁶ G. Hamel de Monchenault,⁶⁶ W. Kozanecki,⁶⁶ G. Vasseur,⁶⁶ Ch. Yèche,⁶⁶ M. Zito,⁶⁶ X. R. Chen,⁶⁷ H. Liu,⁶⁷ W. Park,⁶⁷ M. V. Purohit,⁶⁷ R. M. White,⁶⁷ J. R. Wilson,⁶⁷ M. T. Allen,⁶⁸ D. Aston,⁶⁸ R. Bartoldus,⁶⁸ P. Bechtel,⁶⁸ J. F. Benitez,⁶⁸ R. Cenci,⁶⁸ J. P. Coleman,⁶⁸ M. R. Convery,⁶⁸ J. C. Dingfelder,⁶⁸ J. Dorfan,⁶⁸ G. P. Dubois-Felsmann,⁶⁸ W. Dunwoodie,⁶⁸ R. C. Field,⁶⁸ A. M. Gabareen,⁶⁸ S. J. Gowdy,⁶⁸ M. T. Graham,⁶⁸ P. Grenier,⁶⁸ C. Hast,⁶⁸ W. R. Innes,⁶⁸ J. Kaminski,⁶⁸ M. H. Kelsey,⁶⁸ H. Kim,⁶⁸ P. Kim,⁶⁸ M. L. Kocian,⁶⁸ D. W. G. S. Leith,⁶⁸ S. Li,⁶⁸ B. Lindquist,⁶⁸ S. Luitz,⁶⁸ V. Luth,⁶⁸ H. L. Lynch,⁶⁸ D. B. MacFarlane,⁶⁸ H. Marsiske,⁶⁸ R. Messner,⁶⁸ D. R. Muller,⁶⁸ H. Neal,⁶⁸ S. Nelson,⁶⁸ C. P. O'Grady,⁶⁸ I. Ofte,⁶⁸ A. Perazzo,⁶⁸ M. Perl,⁶⁸ B. N. Ratcliff,⁶⁸ A. Roodman,⁶⁸ A. A. Salnikov,⁶⁸ R. H. Schindler,⁶⁸ J. Schwiening,⁶⁸ A. Snyder,⁶⁸ D. Su,⁶⁸ M. K. Sullivan,⁶⁸ K. Suzuki,⁶⁸ S. K. Swain,⁶⁸ J. M. Thompson,⁶⁸ J. Va'vra,⁶⁸ A. P. Wagner,⁶⁸ M. Weaver,⁶⁸ C. A. West,⁶⁸ W. J. Wisniewski,⁶⁸ M. Wittgen,⁶⁸ D. H. Wright,⁶⁸ H. W. Wulsin,⁶⁸ A. K. Yarritu,⁶⁸ K. Yi,⁶⁸ C. C. Young,⁶⁸ V. Ziegler,⁶⁸ P. R. Burchat,⁶⁹ A. J. Edwards,⁶⁹ S. A. Majewski,⁶⁹ T. S. Miyashita,⁶⁹ B. A. Petersen,⁶⁹ L. Wilden,⁶⁹ S. Ahmed,⁷⁰ M. S. Alam,⁷⁰ J. A. Ernst,⁷⁰ B. Pan,⁷⁰ M. A. Saeed,⁷⁰ S. B. Zain,⁷⁰ S. M. Spanier,⁷¹ B. J. Wogslund,⁷¹ R. Eckmann,⁷² J. L. Ritchie,⁷² A. M. Ruland,⁷² C. J. Schilling,⁷² R. F. Schwitters,⁷² B. W. Drummond,⁷³ J. M. Izen,⁷³ X. C. Lou,⁷³ F. Bianchi,^{74a,74b} D. Gamba,^{74a,74b} M. Pelliccioni,^{74a,74b} M. Bomben,^{75a,75b} L. Bosisio,^{75a,75b} C. Cartaro,^{75a,75b} G. Della Ricca,^{75a,75b} L. Lanceri,^{75a,75b} L. Vitale,^{75a,75b} V. Azzolini,⁷⁶ N. Lopez-March,⁷⁶ F. Martinez-Vidal,⁷⁶ D. A. Milanes,⁷⁶ A. Oyanguren,⁷⁶ J. Albert,⁷⁷ Sw. Banerjee,⁷⁷ B. Bhuyan,⁷⁷ H. H. F. Choi,⁷⁷ K. Hamano,⁷⁷ R. Kowalewski,⁷⁷ M. J. Lewczuk,⁷⁷ I. M. Nugent,⁷⁷ J. M. Roney,⁷⁷ R. J. Sobie,⁷⁷ T. J. Gershon,⁷⁸ P. F. Harrison,⁷⁸ J. Ilic,⁷⁸ T. E. Latham,⁷⁸ G. B. Mohanty,⁷⁸ H. R. Band,⁷⁹ X. Chen,⁷⁹ S. Dasu,⁷⁹ K. T. Flood,⁷⁹ Y. Pan,⁷⁹ M. Pierini,⁷⁹ R. Prepost,⁷⁹ C. O. Vuosalo,⁷⁹ and S. L. Wu⁷⁹

(BABAR Collaboration)

¹Laboratoire de Physique des Particules, IN2P3/CNRS et Université de Savoie, F-74941 Annecy-Le-Vieux, France

²Universitat de Barcelona, Facultat de Física, Departament ECM, E-08028 Barcelona, Spain

^{3a}INFN Sezione di Bari, I-70126 Bari, Italy

^{3b}Dipartimento di Fisica, Università di Bari, I-70126 Bari, Italy

⁴University of Bergen, Institute of Physics, N-5007 Bergen, Norway

⁵Lawrence Berkeley National Laboratory, Berkeley, California 94720, USA, and
University of California, Berkeley, California 94720, USA

⁶University of Birmingham, Birmingham, B15 2TT, United Kingdom

⁷Ruhr Universität Bochum, Institut für Experimentalphysik I, D-44780 Bochum, Germany

⁸University of Bristol, Bristol BS8 1TL, United Kingdom

⁹University of British Columbia, Vancouver, British Columbia, Canada V6T 1Z1

¹⁰Brunel University, Uxbridge, Middlesex UB8 3PH, United Kingdom

¹¹Budker Institute of Nuclear Physics, Novosibirsk 630090, Russia

¹²University of California at Irvine, Irvine, California 92697, USA

¹³University of California at Los Angeles, Los Angeles, California 90024, USA

¹⁴University of California at Riverside, Riverside, California 92521, USA

¹⁵University of California at San Diego, La Jolla, California 92093, USA

¹⁶University of California at Santa Barbara, Santa Barbara, California 93106, USA

¹⁷University of California at Santa Cruz, Institute for Particle Physics, Santa Cruz, California 95064, USA

¹⁸California Institute of Technology, Pasadena, California 91125, USA

¹⁹University of Cincinnati, Cincinnati, Ohio 45221, USA

²⁰University of Colorado, Boulder, Colorado 80309, USA

²¹Colorado State University, Fort Collins, Colorado 80523, USA

²²Technische Universität Dortmund, Fakultät Physik, D-44221 Dortmund, Germany

²³Technische Universität Dresden, Institut für Kern- und Teilchenphysik, D-01062 Dresden, Germany

²⁴Laboratoire Leprince-Ringuet, CNRS/IN2P3, Ecole Polytechnique, F-91128 Palaiseau, France

²⁵University of Edinburgh, Edinburgh EH9 3JZ, United Kingdom

^{26a}INFN Sezione di Ferrara, I-44100 Ferrara, Italy

^{26b}Dipartimento di Fisica, Università di Ferrara, I-44100 Ferrara, Italy

²⁷INFN Laboratori Nazionali di Frascati, I-00044 Frascati, Italy

^{28a}INFN Sezione di Genova, I-16146 Genova, Italy

^{28b}Dipartimento di Fisica, Università di Genova, I-16146 Genova, Italy

²⁹Harvard University, Cambridge, Massachusetts 02138, USA

- ³⁰*Universität Heidelberg, Physikalisches Institut, Philosophenweg 12, D-69120 Heidelberg, Germany*
- ³¹*Humboldt-Universität zu Berlin, Institut für Physik, Newtonstr. 15, D-12489 Berlin, Germany*
- ³²*Imperial College London, London, SW7 2AZ, United Kingdom, USA*
- ³³*University of Iowa, Iowa City, Iowa 52242, USA*
- ³⁴*Iowa State University, Ames, Iowa 50011-3160, USA*
- ³⁵*Johns Hopkins University, Baltimore, Maryland 21218, USA*
- ³⁶*Universität Karlsruhe, Institut für Experimentelle Kernphysik, D-76021 Karlsruhe, Germany*
- ³⁷*Laboratoire de l'Accélérateur Linéaire, IN2P3/CNRS et Université Paris-Sud 11, Centre Scientifique d'Orsay, B. P. 34, F-91898 Orsay Cedex, France*
- ³⁸*Lawrence Livermore National Laboratory, Livermore, California 94550, USA*
- ³⁹*University of Liverpool, Liverpool L69 7ZE, United Kingdom*
- ⁴⁰*Queen Mary, University of London, London, E1 4NS, United Kingdom*
- ⁴¹*University of London, Royal Holloway and Bedford New College, Egham, Surrey TW20 0EX, United Kingdom*
- ⁴²*University of Louisville, Louisville, Kentucky 40292, USA*
- ⁴³*University of Manchester, Manchester M13 9PL, United Kingdom*
- ⁴⁴*University of Maryland, College Park, Maryland 20742, USA*
- ⁴⁵*University of Massachusetts, Amherst, Massachusetts 01003, USA*
- ⁴⁶*Massachusetts Institute of Technology, Laboratory for Nuclear Science, Cambridge, Massachusetts 02139, USA*
- ⁴⁷*McGill University, Montréal, Québec, Canada H3A 2T8*
- ^{48a}*INFN Sezione di Milano, I-20133 Milano, Italy*
- ^{48b}*Dipartimento di Fisica, Università di Milano, I-20133 Milano, Italy*
- ⁴⁹*University of Mississippi, University, Mississippi 38677, USA*
- ⁵⁰*Université de Montréal, Physique des Particules, Montréal, Québec, Canada H3C 3J7*
- ⁵¹*Mount Holyoke College, South Hadley, Massachusetts 01075, USA*
- ^{52a}*INFN Sezione di Napoli, I-80126 Napoli, Italy*
- ^{52b}*Dipartimento di Scienze Fisiche, Università di Napoli Federico II, I-80126 Napoli, Italy*
- ⁵³*NIKHEF, National Institute for Nuclear Physics and High Energy Physics, NL-1009 DB Amsterdam, The Netherlands*
- ⁵⁴*University of Notre Dame, Notre Dame, Indiana 46556, USA*
- ⁵⁵*Ohio State University, Columbus, Ohio 43210, USA*
- ⁵⁶*University of Oregon, Eugene, Oregon 97403, USA*
- ^{57a}*INFN Sezione di Padova, I-35131 Padova, Italy*
- ^{57b}*Dipartimento di Fisica, Università di Padova, I-35131 Padova, Italy*
- ⁵⁸*Laboratoire de Physique Nucléaire et de Hautes Energies, IN2P3/CNRS, Université Pierre et Marie Curie-Paris6, Université Denis Diderot-Paris7, F-75252 Paris, France*
- ⁵⁹*University of Pennsylvania, Philadelphia, Pennsylvania 19104, USA*
- ^{60a}*INFN Sezione di Perugia, I-06100 Perugia, Italy*
- ^{60b}*Dipartimento di Fisica, Università di Perugia, I-06100 Perugia, Italy*
- ^{61a}*INFN Sezione di Pisa, I-56127 Pisa, Italy*
- ^{61b}*Dipartimento di Fisica, Università di Pisa, I-56127 Pisa, Italy*
- ^{61c}*Scuola Normale Superiore di Pisa, I-56127 Pisa, Italy*
- ⁶²*Princeton University, Princeton, New Jersey 08544, USA*
- ^{63a}*INFN Sezione di Roma, I-00185 Roma, Italy*
- ^{63b}*Dipartimento di Fisica, Università di Roma La Sapienza, I-00185 Roma, Italy*
- ⁶⁴*Universität Rostock, D-18051 Rostock, Germany*
- ⁶⁵*Rutherford Appleton Laboratory, Chilton, Didcot, Oxon, OX11 0QX, United Kingdom*
- ⁶⁶*DSM/Irfu, CEA/Saclay, F-91191 Gif-sur-Yvette Cedex, France*
- ⁶⁷*University of South Carolina, Columbia, South Carolina 29208, USA*
- ⁶⁸*Stanford Linear Accelerator Center, Stanford, California 94309, USA*
- ⁶⁹*Stanford University, Stanford, California 94305-4060, USA*
- ⁷⁰*State University of New York, Albany, New York 12222, USA*
- ⁷¹*University of Tennessee, Knoxville, Tennessee 37996, USA*
- ⁷²*University of Texas at Austin, Austin, Texas 78712, USA*
- ⁷³*University of Texas at Dallas, Richardson, Texas 75083, USA*
- ^{74a}*INFN Sezione di Torino, I-10125 Torino, Italy*
- ^{74b}*Dipartimento di Fisica Sperimentale, Università di Torino, I-10125 Torino, Italy*
- ^{75a}*INFN Sezione di Trieste, I-34127 Trieste, Italy*
- ^{75b}*Dipartimento di Fisica, Università di Trieste, I-34127 Trieste, Italy*
- ⁷⁶*IFIC, Universitat de Valencia-CSIC, E-46071 Valencia, Spain*
- ⁷⁷*University of Victoria, Victoria, British Columbia, Canada V8W 3P6*
- ⁷⁸*Department of Physics, University of Warwick, Coventry CV4 7AL, United Kingdom*

⁷⁹University of Wisconsin, Madison, Wisconsin 53706, USA
(Received 19 July 2008; published 13 October 2008)

We measure the time-dependent CP asymmetry in $B^0 \rightarrow K_S^0 \pi^0 \gamma$ decays for two regions of $K_S^0\text{-}\pi^0$ invariant mass, $m(K_S^0 \pi^0)$, using the final *BABAR* data set of 467×10^6 $B\bar{B}$ pairs collected at the PEP-II e^+e^- collider at SLAC. We find 339 ± 24 $B^0 \rightarrow K^{*0} \gamma$ candidates and measure $S_{K^{*0}\gamma} = -0.03 \pm 0.29 \pm 0.03$ and $C_{K^{*0}\gamma} = -0.14 \pm 0.16 \pm 0.03$. In the range $1.1 < m(K_S^0 \pi^0) < 1.8$ GeV/ c^2 we find 133 ± 20 $B^0 \rightarrow K_S^0 \pi^0 \gamma$ candidates and measure $S_{K_S^0 \pi^0 \gamma} = -0.78 \pm 0.59 \pm 0.09$ and $C_{K_S^0 \pi^0 \gamma} = -0.36 \pm 0.33 \pm 0.04$. The uncertainties are statistical and systematic, respectively.

DOI: [10.1103/PhysRevD.78.071102](https://doi.org/10.1103/PhysRevD.78.071102)

PACS numbers: 13.20.He, 11.30.Er, 14.40.Nd

The radiative decay $b \rightarrow s \gamma$ serves as a probe of physics beyond the standard model (SM). In the SM it proceeds at leading order through a loop diagram, making it sensitive to possible virtual contributions from as yet undiscovered particles. Because of parity violation in the weak interaction, the photon in $b \rightarrow s \gamma$ is predominantly left-handed, while it is right-handed in the charge-conjugate decay. The photon polarization can be determined indirectly through a measurement of time-dependent CP asymmetry in certain neutral decay channels. A nonzero asymmetry S due to interference between B^0 mixing and decay diagrams is only present if both photon helicities contribute to both B^0 and \bar{B}^0 decays [1]. S is expected to be approximately -0.02 in the SM [1,2], though hadronic corrections might permit it to be as large as ± 0.1 [3]. Several new physics scenarios yield large values of the asymmetry; these include left-right symmetric models [1,4] and supersymmetric models [5]. Because the SM asymmetry is small, any significant evidence of a large asymmetry would point to a source beyond the SM.

We present an updated measurement of the time-dependent CP asymmetry in $B^0 \rightarrow K_S^0 \pi^0 \gamma$ based on the final *BABAR* data set of 467×10^6 $Y(4S) \rightarrow B\bar{B}$ decays collected at the PEP-II asymmetric-energy e^+e^- storage rings at SLAC. Previous measurements have been performed by *BABAR* [6] and Belle [7]. Changes since *BABAR*'s last published result include doubling the data set, improved track reconstruction, better removal of background photons from π^0 and η decays, better rejection of $B^+ \rightarrow K^{*+} \gamma$ background [8], and an improved evaluation of the systematic uncertainties from nonsignal B decays. At leading order in the SM, the CP asymmetries of this mode do not depend on $m(K_S^0 \pi^0)$ [9]. However, since

the aforementioned hadronic corrections [3] or new physics could introduce this dependence, we split the data into two parts: the K^* region with $0.8 < m(K_S^0 \pi^0) < 1.0$ GeV/ c^2 and the non- K^* region with $1.1 < m(K_S^0 \pi^0) < 1.8$ GeV/ c^2 .

Time-dependent CP asymmetries are determined using the difference of B^0 meson proper decay times $\Delta t = t_{\text{sig}} - t_{\text{tag}}$, where t_{sig} is the proper decay time of the signal $B^0 \rightarrow K_S^0 \pi^0 \gamma$ candidate (B_{sig}) and t_{tag} is that of the other B (B_{tag}), which is partially reconstructed and flavor-tagged based on its daughter tracks. The Δt distribution for B_{sig} decaying to a CP eigenstate is

$$\mathcal{P}_{\pm}(\Delta t) = \frac{e^{-|\Delta t|/\tau}}{4\tau} [1 \pm S \sin(\Delta m \Delta t) \mp C \cos(\Delta m \Delta t)], \quad (1)$$

where the upper and lower signs correspond to B_{tag} having flavor B^0 and \bar{B}^0 respectively, τ is the B^0 lifetime, and Δm is the $B^0\text{-}\bar{B}^0$ mixing frequency. The C coefficient corresponds to the direct CP asymmetry in decay, expected to be smaller than 1% in the SM [10].

We evaluate our selection criteria with a detailed Monte Carlo (MC) simulation of the *BABAR* detector [11], using the EVTGEN generator [12] and the GEANT4 package [13]. We require photon candidates to have energy greater than 30 MeV and the expected lateral shower shapes in the electromagnetic calorimeter (EMC). The primary photon from the B decay must be isolated by more than 25 cm from other charged and neutral clusters in the EMC. Primary-photon candidates that make a π^0 or η candidate when combined with another photon in the event are discarded based on a likelihood formed from the diphoton mass and the energy of the second photon. We select $K_S^0 \rightarrow \pi^+ \pi^-$ candidates from oppositely-charged tracks for which the probability of a geometrical vertex fit is greater than 0.1%, the $\pi^+ \pi^-$ invariant mass is between 487 and 508 MeV/ c^2 , and the reconstructed decay length is greater than 5 times its uncertainty. We select $\pi^0 \rightarrow \gamma \gamma$ candidates with invariant mass between 115 and 155 MeV/ c^2 and energy greater than 590 MeV in the laboratory frame. For candidates in the K^* region we require $|\cos \theta_{K^*}| < 0.9$, where θ_{K^*} is the angle between the K_S^0 and primary photon direction in the K^* rest frame.

*Deceased.

[†]Now at Temple University, Philadelphia, Pennsylvania 19122, USA.

[‡]Now at Tel Aviv University, Tel Aviv, 69978, Israel.

[§]Also with Università di Perugia, Dipartimento di Fisica, Perugia, Italy.

^{||}Also with Università di Roma La Sapienza, I-00185 Roma, Italy.

[¶]Now at University of South Alabama, Mobile, Alabama 36688, USA.

^{**}Also with Università di Sassari, Sassari, Italy.

To identify signal decays we use the energy-substituted mass $m_{\text{ES}} = \sqrt{(s/2c^2 + \mathbf{p}_0 \cdot \mathbf{p}_B)^2/E_0^2 - |\mathbf{p}_B|^2/c^2}$ and the energy difference $\Delta E = E_B^* - \sqrt{s}/2$, where $(E_0/c, \mathbf{p}_0)$ and $(E_B/c, \mathbf{p}_B)$ are the four-momenta of the initial e^+e^- system and the B candidate, respectively, \sqrt{s} is the center-of-mass (CM) energy, and the asterisk denotes the CM frame. The distributions of signal events show a peak in these variables. We require $5.2 < m_{\text{ES}} < 5.3 \text{ GeV}/c^2$ and $|\Delta E| < 250 \text{ MeV}$. To reduce $B^+ \rightarrow K^{*+} \gamma$ background, we reconstruct $B^+ \rightarrow K^{*+}(K_S^0 \pi^+) \gamma$ candidates subject to the same requirements as B^0 candidates, and veto events for which $m_{\text{ES}}(B^+) > 5.27 \text{ GeV}/c^2$ and $0.8 < m(K_S^0 \pi^+) < 1.0 \text{ GeV}/c^2$. To discriminate B decays from continuum $e^+e^- \rightarrow q\bar{q}$ ($q = u, d, s, c$) background, we require $|\cos\theta_B^*| < 0.9$, where θ_B^* is the CM angle between the B candidate and the e^- beam direction. We require the ratio of event-shape moments L_2/L_0 to be less than 0.55, where $L_i = \sum_j |p_j^i| |\cos\theta_j^*|^i$, p_j^i is the CM momentum of each particle j not used to reconstruct the B candidate, and θ_j^* is the CM angle between p_j^i and the thrust axis of the reconstructed B candidate. After all selection criteria have been applied we find 10 587 candidate events, 16% of which have more than one signal B^0 candidate. In these cases we select the one with π^0 mass closest to its nominal value [14], and if there is still an ambiguity, we select the one with the K_S^0 mass closest to its nominal value. We find an overall selection efficiency of 16%.

For each reconstructed signal candidate we use the remaining tracks in the event to determine the decay vertex position and flavor of B_{tag} . The latter is determined by a neural network based on kinematic and particle identification information, the performance of which is evaluated using a sample of fully reconstructed, self-tagging hadronic B^0 decays (B_{flav} sample) [15].

We determine the proper time difference between B_{sig} and B_{tag} from the spatial separation between their decay vertices in the same way as our previous analysis and a similar *BABAR* study of $B^0 \rightarrow K_S^0 \pi^0$ [16]. Because both the transverse flight length of the B^0 mesons and the transverse size of the interaction region are small compared to the B^0 flight length along the boost direction, we are able to determine a decay vertex from the intersection of the K_S^0 trajectory with the interaction region. We further improve the Δt resolution by 11% over what is obtained using information from the interaction region alone by refitting the $Y(4S) \rightarrow B^0 \bar{B}^0$ system with the constraint that the average sum of decay times ($t_{\text{sig}} + t_{\text{tag}}$) be equal to twice the B lifetime with an uncertainty of $\sqrt{2}\tau_B$. Using MC simulation data we verify that this procedure gives an unbiased estimate of Δt . We define events as having good Δt quality if each pion daughter of the K_S^0 creates at least 2 hits in the silicon vertex tracker (SVT), and if the Δt uncertainty $\sigma_{\Delta t} < 2.5 \text{ ps}$ and $|\Delta t| < 20 \text{ ps}$. About 70% of signal and background events pass these requirements. We

split our data set and fitting procedure based on the Δt quality such that flavor-tagged events with poor Δt information do not contribute to the measurement of S , but do contribute to the measurement of C , which can be determined solely through tagging.

We extract signal yields and CP asymmetries using an unbinned maximum likelihood fit to m_{ES} , ΔE , L_2/L_0 , tag flavor, Δt , $\sigma_{\Delta t}$, and, in the K^* region, $m(K_S^0 \pi^0)$. Continuum and $B\bar{B}$ backgrounds are also modeled in the fit. We construct the likelihood function for each contribution as the product of one-dimensional probability density functions (PDFs). The signal PDFs in m_{ES} and ΔE are parametrized using the function

$$f(x) = \exp\left[\frac{-(x - \mu)^2}{2\sigma^2 + \alpha(x - \mu)^2}\right], \quad (2)$$

where μ is the mean, σ the core width, and α a tail parameter. The latter two parameters are allowed to be different on either side of the peak. The signal $m(K_S^0 \pi^0)$ shape is a relativistic Breit-Wigner, as nonresonant contributions in the K^* region are negligible [17]. For continuum m_{ES} we use an ARGUS [18] function, while for ΔE we use an exponential shape. The continuum and $B\bar{B}$ shape in $m(K_S^0 \pi^0)$ is a Breit-Wigner on top of a linear background. We parametrize the $B\bar{B}$ m_{ES} shape as the sum of an ARGUS function and a Gaussian with different widths below and above the peak, and the ΔE shape as an exponential. The L_2/L_0 shapes are binned PDFs, and in those the signal and $B\bar{B}$ components share the same parameters. All signal and $B\bar{B}$ PDF parameters are determined using simulated events, except for the flavor tag efficiencies, mistag probabilities, and Δt resolution function parameters, which are determined from the B_{flav} sample. The large number of continuum background events in the fit determine the continuum PDF parameters.

We obtain the Δt PDF for signal events and $B\bar{B}$ background from Eq. (1), accounting for the mistag probability and convolving with the Δt resolution function, which is the sum of three Gaussian distributions [15]. The effective CP asymmetries for the $B\bar{B}$ background, $S_{B\bar{B}}^{\text{bkg}}$ and $C_{B\bar{B}}^{\text{bkg}}$, are fixed to zero in the fit, and we account for a possible deviation from zero in the systematic uncertainty. We verify in simulation that the parameters of the resolution function for signal events are compatible with those obtained from the B_{flav} sample. Therefore we use the B_{flav} parameters for better precision. We fit the continuum MC Δt distribution and find that it is well-modeled by a prompt decay distribution consisting only of the Δt resolution function shape. The parameters of the continuum Δt PDF are determined in the fit to data.

In the fit to the $B^0 \rightarrow K^{*0} \gamma$ candidate sample of 3884 events we find $339 \pm 24(\text{stat})$ signal events, $S_{K^* \gamma} = -0.03 \pm 0.29(\text{stat}) \pm 0.03(\text{syst})$ and $C_{K^* \gamma} = -0.14 \pm 0.16(\text{stat}) \pm 0.03(\text{syst})$. We also find $19 \pm 27(\text{stat})$ $B\bar{B}$

background events. In the range $1.1 < m(K_S^0 \pi^0) < 1.8 \text{ GeV}/c^2$ with 6703 events we measure $133 \pm 20(\text{stat})$ signal events, $S_{K_S^0 \pi^0 \gamma} = -0.78 \pm 0.59(\text{stat}) \pm 0.09(\text{syst})$ and $C_{K_S^0 \pi^0 \gamma} = -0.36 \pm 0.33(\text{stat}) \pm 0.04(\text{syst})$. We find $167 \pm 49(\text{stat})$ $B\bar{B}$ background events in this sample. The linear correlation coefficient between $S_{K^* \gamma}$ and $C_{K^* \gamma}$ is $+0.050$, while for $S_{K_S^0 \pi^0 \gamma}$ and $C_{K_S^0 \pi^0 \gamma}$ it is $+0.015$. Figure 1 shows signal-enhanced distributions for m_{ES} and ΔE created by cutting on the likelihood of the unplotted fit variables.

We perform a cross-check because of the discrepancy between the projection of the fit model and the data in the non- K^* region at low m_{ES} . A fit of the data sample with $m_{\text{ES}} > 5.22 \text{ GeV}/c^2$ shows that the observed changes in S and C are consistent with statistical fluctuations, so the signal is not significantly affected. Additionally, we verified that the slope of the m_{ES} background shape is not correlated with the other fit variables. MC simulations of common $B\bar{B}$ backgrounds, including the final states $K_S^0 \pi \pi \gamma$ and $K_S^0 \pi \pi \pi^0$, do not show any rising structure at low m_{ES} .

Figure 2 shows the background-subtracted distributions of Δt in the K^* region, obtained with the sPlot event weighting technique [19]. We show an sPlot of the $m(K_S^0 \pi^0)$ spectrum in Fig. 3.

Using an ensemble of simulated experiments generated from the fitted likelihood function we find no bias in the K^* region and a spread in S and C consistent with the statistical uncertainties. In the non- K^* region we find a bias of -0.06 ± 0.03 on S and a spread in C larger than the statistical uncertainty reported by the fit. These effects are due to a measurement that is close to the physical boundary of $S^2 + C^2 \leq 1$, and they disappear if we generate the ensemble with $S_{K_S^0 \pi^0 \gamma} = C_{K_S^0 \pi^0 \gamma} = 0$. The bias on $S_{K_S^0 \pi^0 \gamma}$ is evaluated with several ensembles of simulated events in which the generated $S_{K_S^0 \pi^0 \gamma}$ is varied. For the statistical uncertainty on C we take the ensemble's root-mean-square width of 0.33 instead of the 0.29 uncertainty determined by the fit to data.

Systematic uncertainties associated with our knowledge of the beam spot position and possible SVT misalignment are determined by varying the beam spot and SVT alignment parameters in MC. We bound the effects of uncertainties in the Δt resolution function due to the vertexing method with a study from *BABAR*'s $B^0 \rightarrow K_S^0 \pi^0$ analysis [20]. Resolution function differences between data and MC in control samples of $B^0 \rightarrow J/\psi K_S^0$ decays, in which the J/ψ vertex information is ignored, lead to differences in S and C that we take as systematic uncertainties. Un-

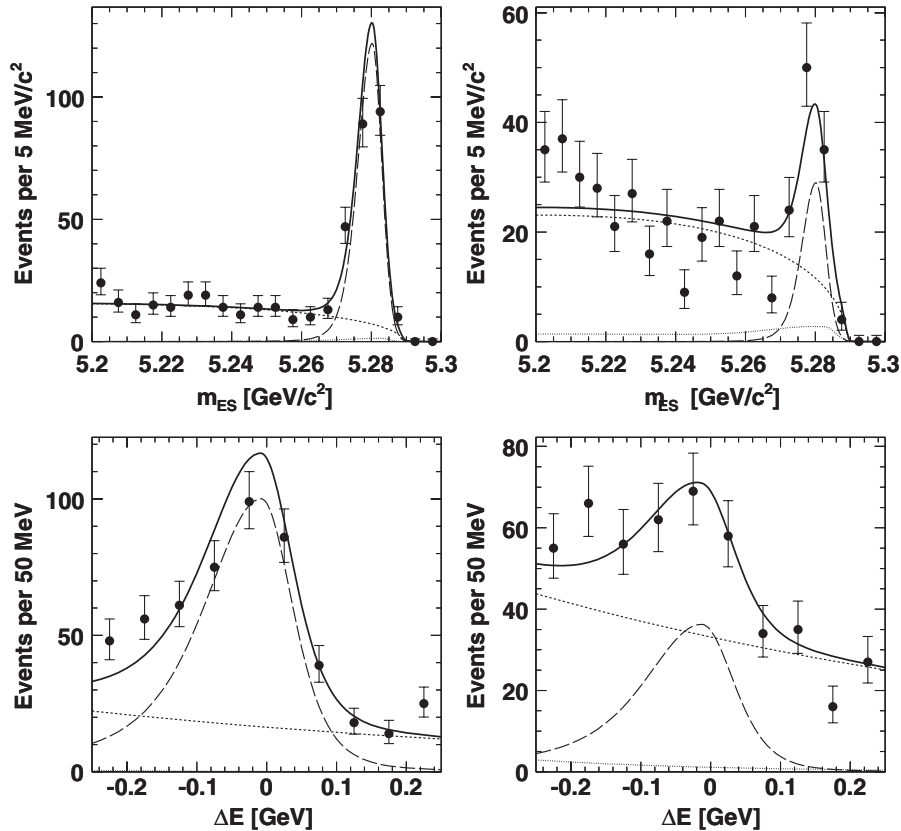


FIG. 1. Signal-enhanced distributions for m_{ES} (top) and ΔE (bottom) for the K^* region (left) and the non- K^* region (right). We show the fit result (solid line) and PDFs for signal (long dashed line), continuum (short dashed line), and $B\bar{B}$ (dotted line).

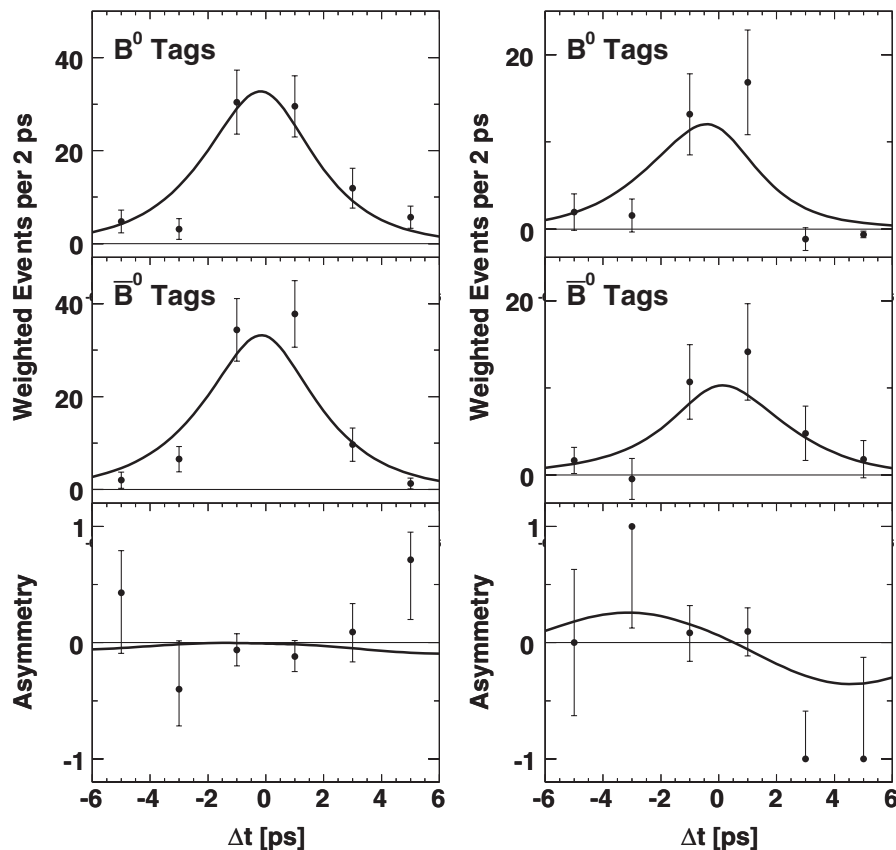


FIG. 2. sPlot (see text) of Δt in the K^* region (left) and the non- K^* region (right), with B_{tag} tagged as B^0 (top) or \bar{B}^0 (center), and the asymmetry (bottom). The curves are the signal PDFs.

certainties from doubly-Cabibbo-suppressed (DCS) decays of the B_{tag} are included as in Ref. [15].

We evaluate uncertainties due to the vertex reconstruction procedure and possible correlations among the observables with an ensemble of simulated experiments created by generating background events from the PDFs and embedding signal events from the full MC simulation. No significant bias is observed in the K^* region, and we bound uncertainties by the precision with which the potential bias is measured. In the non- K^* region, no bias is observed in the signal MC.

Uncertainties due to limited knowledge of the fixed parameters in the fit are evaluated by varying them within their uncertainties. We evaluate differences between data and MC in the signal shape by fixing the background parameters to those determined in the fit to data and floating the signal parameters separately for each observable.

We evaluate the effect of $S_{B\bar{B}}^{\text{bkg}}$ and $C_{B\bar{B}}^{\text{bkg}}$ by varying them over a range determined by the composition of the $B\bar{B}$ background samples and CP asymmetry measurements in the PDG listings. The systematic uncertainties are summarized in Table I.

In summary, we have measured the time-dependent CP asymmetry in $B^0 \rightarrow K_S^0 \pi^0 \gamma$ decays using the full BABAR data set recorded at the $\Upsilon(4S)$ resonance. We find

$$S_{K^* \gamma} = -0.03 \pm 0.29(\text{stat}) \pm 0.03(\text{syst}),$$

$$C_{K^* \gamma} = -0.14 \pm 0.16(\text{stat}) \pm 0.03(\text{syst}),$$

$$S_{K_S^0 \pi^0 \gamma} = -0.78 \pm 0.59(\text{stat}) \pm 0.09(\text{syst}),$$

$$C_{K_S^0 \pi^0 \gamma} = -0.36 \pm 0.33(\text{stat}) \pm 0.04(\text{syst}).$$

The measurement in each $m(K_S^0 \pi^0)$ region is consistent within uncertainties with the predictions of the standard model.

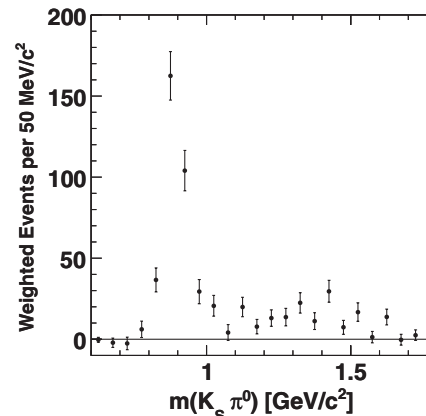


FIG. 3. sPlot (see text) of $m(K_S^0 \pi^0)$.

TABLE I. Summary of systematic uncertainties.

Source	K^* region		non- K^* region	
	ΔS	ΔC	ΔS	ΔC
Beamspot	0.007	0.002	0.007	0.002
SVT alignment	0.010	0.010	0.010	0.010
Resolution function	0.011	0.018	0.011	0.018
Bias uncertainty	0.015	0.009	0.028	0.016
PDF uncertainty	0.015	0.013	0.060	0.019
$S_{B\bar{B}}^{\text{bkg}}$ and $C_{B\bar{B}}^{\text{bkg}}$	0.008	0.002	0.060	0.018
DCS B_{tag} decays	0.001	0.015	0.001	0.015
Total	0.028	0.030	0.091	0.040

We are grateful for the excellent luminosity and machine conditions provided by our PEP-II colleagues, and for the substantial dedicated effort from the computing organizations that support *BABAR*. The collaborating institutions wish to thank SLAC for its support and kind hospitality. This work is supported by DOE and NSF (USA), NSERC

(Canada), CEA and CNRS-IN2P3 (France), BMBF and DFG (Germany), INFN (Italy), FOM (The Netherlands), NFR (Norway), MES (Russia), MEC (Spain), and STFC (United Kingdom). Individuals have received support from the Marie Curie EIF (European Union) and the A. P. Sloan Foundation.

-
- [1] D. Atwood, M. Gronau, and A. Soni, *Phys. Rev. Lett.* **79**, 185 (1997).
- [2] M. Matsumori and A. I. Sanda, *Phys. Rev. D* **73**, 114022 (2006); P. Ball and R. Zwicky, *Phys. Lett. B* **642**, 478 (2006).
- [3] B. Grinstein, Y. Grossman, Z. Ligeti, and D. Pirjol, *Phys. Rev. D* **71**, 011504(R) (2005); B. Grinstein and D. Pirjol, *Phys. Rev. D* **73**, 014013 (2006).
- [4] D. Cocolicchio, G. Costa, G. L. Fogli, J. H. Kim, and A. Masiero, *Phys. Rev. D* **40**, 1477 (1989); K. Fujikawa and A. Yamada, *Phys. Rev. D* **49**, 5890 (1994); K. S. Babu, K. Fujikawa, and A. Yamada, *Phys. Lett. B* **333**, 196 (1994); P. L. Cho and M. Misiak, *Phys. Rev. D* **49**, 5894 (1994).
- [5] E. J. Chun, K. Hwang, and J. S. Lee, *Phys. Rev. D* **62**, 076006 (2000); L. L. Everett, G. L. Kane, S. Rigolin, L. T. Wang, and T. T. Wang, *J. High Energy Phys.* 01 (2002) 022; C. K. Chua, W. S. Hou, and M. Nagashima, *Phys. Rev. Lett.* **92**, 201803 (2004); T. Goto, Y. Okada, T. Shindou, and M. Tanaka, *Phys. Rev. D* **77**, 095010 (2008).
- [6] B. Aubert *et al.* (*BABAR* Collaboration), *Phys. Rev. D* **72**, 051103 (2005).
- [7] Y. Ushiroda *et al.* (Belle Collaboration), *Phys. Rev. D* **74**, 111104 (2006).
- [8] Unless explicitly stated, charge-conjugate decay modes are included implicitly throughout this paper.
- [9] D. Atwood, T. Gershon, M. Hazumi, and A. Soni, *Phys. Rev. D* **71**, 076003 (2005).
- [10] J. M. Soares, *Nucl. Phys.* **B367**, 575 (1991); A. L. Kagan and M. Neubert, *Phys. Rev. D* **58**, 094012 (1998).
- [11] B. Aubert *et al.* (*BABAR* Collaboration), *Nucl. Instrum. Methods Phys. Res., Sect. A* **479**, 1 (2002).
- [12] D. J. Lange, *Nucl. Instrum. Methods Phys. Res., Sect. A* **462**, 152 (2001).
- [13] S. Agostinelli *et al.* (GEANT4 Collaboration), *Nucl. Instrum. Methods Phys. Res., Sect. A* **506**, 250 (2003).
- [14] W. M. Yao *et al.* (Particle Data Group), *J. Phys. G* **33**, 1 (2006).
- [15] B. Aubert *et al.* (*BABAR* Collaboration), *Phys. Rev. Lett.* **99**, 171803 (2007).
- [16] B. Aubert *et al.* (*BABAR* Collaboration), *Phys. Rev. Lett.* **93**, 131805 (2004).
- [17] M. Nakao *et al.* (Belle Collaboration), *Phys. Rev. D* **69**, 112001 (2004); B. Aubert *et al.* (*BABAR* Collaboration), *Phys. Rev. D* **70**, 112006 (2004).
- [18] H. Albrecht *et al.* (ARGUS Collaboration), *Z. Phys. C* **48**, 543 (1990).
- [19] M. Pivk and F. R. Le Diberder, *Nucl. Instrum. Methods Phys. Res., Sect. A* **555**, 356 (2005).
- [20] B. Aubert *et al.* (*BABAR* Collaboration), *Phys. Rev. D* **77**, 012003 (2008).